(DMEM containing 2% FCS and 10 mM HEPES (Sigma)) and subsequently divided into two portions. After incubation in incubation medium for 90 min at 37 °C, (*R*)+-verapamil (Sigma, St. Louis, MO) or tryprostatin A (TPS-A; provided by Dr. H. Osada (RIKEN Institute)) was added to one portion (final concentration: 50 μM), after which both portions were incubated for a further 30 min at 37 °C. Antibody-mediated inhibition assay using anti-ABCG2 monoclonal antibody (5D3; eBioscience, San Diego, CA) or isotype control (mouse IgG_{2b}; eBioscience) was performed as previously described [22]. Hoechst 33342 dye (Sigma) was then added to both portions (final concentration: 3 μg/ml), and incubation continued for another 90 min at 37 °C. After the final incubation, cells were kept on ice and analyzed for Hoechst 33342 dye efflux by EPICS Altra FACS analysis (Beckman Coulter, Fullerton, CA). Prior to analysis, propidium iodide (Sigma) was added (final concentration: 2 μg/ml) to distinguish live from dead cells. Hoechst 33342 dye was excited at 350 nm using a UV laser. Fluorescence emission was detected through 450 nm BP (Hoechst blue) and 675 nm LP (Hoechst red) filters, respectively. Propidium iodide in cells was excited at 488 nm (argon ion laser) and fluorescence emission was detected through a 610 nm BP filter.

2.3. Real-time quantitative RT-PCR analysis

SP and non-SP cells were isolated from limbal epithelial cells using EPICS Altra flow cytometric sorting. Total RNA was obtained from equal numbers (2000–3000) of SP and non-SP cells according to the manufacturer's instructions (Isogen; Nippongene, Tokyo, Japan). After DNase I (Invitrogen) treatment, total cellular RNA was divided into two portions. One portion was reverse transcribed with oligo$(dT)_{12-18}$, according to the manufacturer's instructions (SuperScript First-Strand Synthesis System for RT-PCR; Invitrogen), and a 1/10 volume (2 μl) of synthesized cDNA was used as a template for PCR. The other portion was treated in the same manner except for the omission of SuperScript II reverse transcriptase (Invitrogen). The oligonucleotide primers (Invitrogen) used for ABCG2 amplification were 5′-GGTTTCCAAGCGTTCATTCAAA-3′ (forward) and 5′-TAGCCCAAAGTAAATGGCACCTA-3′ (reverse), with an expected product length of 111 bp. The TaqMan probe (Applied Biosystems, Foster City, CA) used for ABCG2 detection was 5′-CCCAGGCCTCTATAGCTCAGATCATTGTCA-3′, labeled with 6-carboxyfluorescein (FAM) at the 5′-end, and with 6-carboxytetraethylrodamine (TAMRA) at the 3′-end. Quantitative PCR was performed using ABI Prism 7900HT Sequence Detection System (Applied Biosystems), according to the manufacturer's instructions. The reaction mixture (30 μl) contained 15 μl of TaqMan Universal PCR Mastermix (Applied Biosystems), 15 pmol of forward and reverse primers, 7.5 pmol of TaqMan probe and 2 μl of the investigated sample. Glyceraldehyde-3-phosphate dehydrogenase (GAPDH) expression was measured using TaqMan GAPDH Control Reagents (Applied Biosystems), according to the manufacturer's instructions. Thermocycling used 50 cycles at 95 °C for 15 s and 60 °C for 1 min with an initial cycle at 50 °C for 2 min and 95 °C for 10 min. A negative control with non-reverse transcribed total RNA as a template was included in every experiment. All assays were run in duplicate. To represent the ABCG2 mRNA expression level, we used the ABCG2 mRNA expression index as the value of the ABCG2 gene copies divided by the value of the housekeeping GAPDH gene copies.

2.4. Statistical analysis

Statistics were calculated using SigmaStat 2.0 (SPSS, Chicago, IL). To compare ABCG2 expression between SP and non-SP cells, the Mann–Whitney rank sum test was applied.

2.5. Immunofluorescence

Cryostat sections (20 μm) were cut from the limbus and from the cornea, dried for 1 h at room temperature, and fixed in acetone for 10 min also at room temperature. Immunofluorescence was performed using DakoCytomation CSA II (DakoCytomation, Kyoto, Japan). Briefly, endogenous peroxidase activity was blocked with 3% hydrogen peroxide in water for 15 min. The slides were first incubated with serum-free protein in buffer for 15 min to block non-specific binding of antibodies, then incubated at 4 °C overnight with a 1:2500 dilution of BXP-21 monoclonal antibody (MBL, Aichi, Japan). BXP-21 was diluted in tris-buffered saline containing 1% bovine serum albumin and 0.1% Tween 20. After incubation, slides were incubated for 15 min with anti-mouse immunoglobulins-HRP, followed by 15 min in fluorescyl-tyramide hydrogen peroxide in buffer. After counterstaining with propidium iodide (Sigma), slides were mounted and observed on a confocal laser scanning microscope (LSM 510 META; Carl Zeiss, Jena, Germany). For each type of tissue, identically treated negative controls were included using normal non-specific IgG_{2a} (DakoCytomation).

3. Results

3.1. SP cells are present in human limbal epithelium

In the Hoechst 33342 dye exclusion assay, a distinct population of cells with a low Hoechst 33342 blue/red fluorescence was detected in epithelial cells from the limbus (Fig. 1A; 0.20% gated cells) but not in cells from the cornea (Fig. 1B, 1D; 0.02% gated cells). Generation of this subpopulation was not seen in the presence of (*R*)+-verapamil, the specific inhibitor of Hoechst 33342 dye transport (Fig. 1C; 0.01% gated cells). These observations indicate that the limbal epithelium contains SP cells.

3.2. Effect of 5D3 and TPS-A on Hoechst 33342 dye efflux

When SP cells were incubated with an anti-ABCG2 monoclonal antibody, 5D3, recognizing an external plasma membrane epitope on living cells [13,22], prior to Hoechst 33342 dye exclusion assay, a marked decrease in SP cell dye efflux was observed (Fig. 2A). Hoechst 33342 dye efflux activity was also inhibited by a novel ABCG2 inhibitor, TPS-A (Fig. 2B), that is known not to inhibit another important ATP-binding cassette transporter, P-glycoprotein [23]. These data strongly suggest that ABCG2 is a major contributor to the SP phenotype of limbal epithelial cells.

3.3. ABCG2 mRNA expression in SP and non-SP cells

To investigate the link between the SP phenotype and ABCG2 expression, SP and non-SP cells from limbal epithelial tissues were analyzed for ABCG2 gene expression by TaqMan real-time

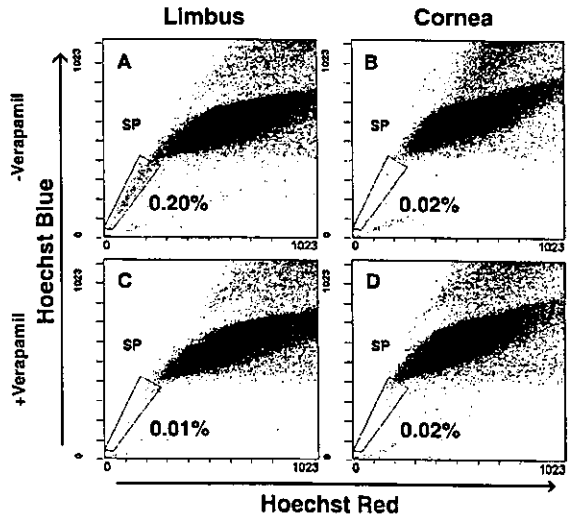

Fig. 1. Flow cytometric analysis of epithelial cells harvested from the limbus and from the cornea. Epithelial cells were isolated from eye bank limbus and cornea tissues, and analyzed for Hoechst 33342 dye efflux by FACS. (A) SP cells were detected in limbal epithelial cells after Hoechst 33342 dye staining. (B) SP cells were absent in corneal epithelial cells. (C) Dye efflux from SP cells was inhibited by verapamil. (D) Verapamil had no effect on dye efflux.

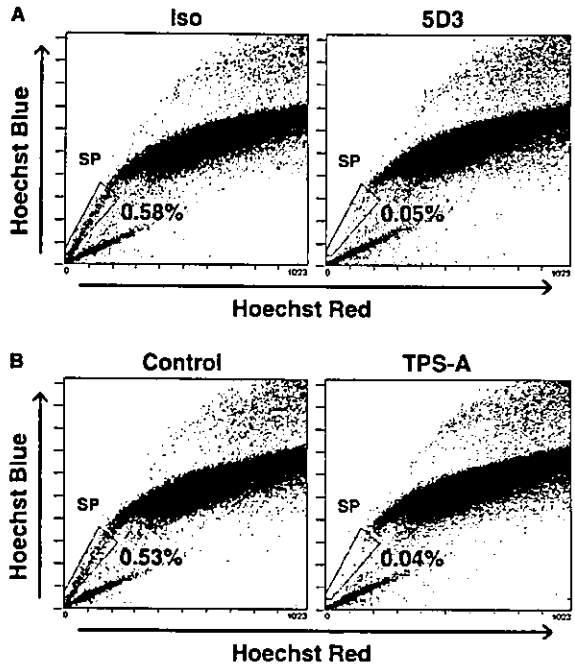

Fig. 2. Influence of ABCG2 inhibitors on the SP phenotype of limbal epithelial cells. Limbal epithelial cells were analyzed for Hoechst 33342 dye efflux in the presence of ABCG2 inhibitors. Dye efflux from SP cells was effectively inhibited by 5D3 monoclonal antibody (A) and by TPS-A (B).

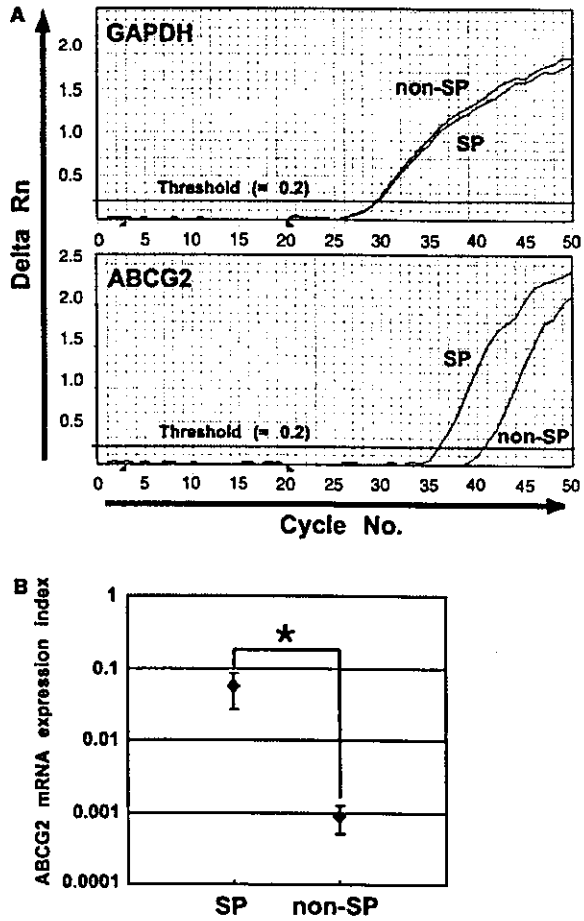

Fig. 3. Quantification of ABCG2 mRNA in SP and non-SP cells. (A) Amplification plots from real-time RT-PCR analysis. Delta Rn is plotted against cycle number. Horizontal red lines show the threshold used for calculation of ABCG2 expression indices. Real-time quantitative RT-PCR procedures were as described in Section 2. (B) ABCG2 mRNA expression indices in SP and non-SP cells. The relative expression of ABCG2 gene was normalized to that of GAPDH in each sample. Data represent the mean value from four samples. Error bars indicate the S.E. ABCG2 mRNA expression in SP cells was significantly higher than in non-SP cells ($P = 0.029$).

RT-PCR (Fig. 3A). ABCG2 mRNA expression indices were $5.61 \times 10^{-2} \pm 2.92 \times 10^{-2}$ (SP) and $8.66 \times 10^{-4} \pm 3.56 \times 10^{-4}$ (non-SP) ($n = 4$, mean ± S.E.) (Fig. 3B). Statistical analysis showed that the ABCG2 mRNA expression level in SP cells was significantly higher than in non-SP cells ($P = 0.029$).

3.4. Distribution of ABCG2-expressing cells

Our immunofluorescence data using BXP-21 monoclonal antibody specific for human ABCG2 revealed that ABCG2 is expressed in the limbal epithelial basal cells (Fig. 4A, B), but not in corneal epithelial cells (Fig. 4C). Observed ABCG2 expression in basal cells is inconsistent and discontinuous in the epithelium, and does not persist throughout the entire limbus (Fig. 4A). Fig. 4B shows that positive staining cells are present not only in the basal but also in the suprabasal cells.

4. Discussion

Corneal epithelial stem cell deficiency caused by ocular trauma or diseases causes corneal opacification and visual loss. Patients with corneal epithelial stem cell deficiency can be treated with autologous or allogenic limbal transplantation [24,25]. However, autologous limbal transplantation requires a large limbal withdrawal from the patient's eye, and allogenic limbal transplantation has a significant risk of rejection. Moreover, shortage of donor tissues is a serious current challenge. To avoid these problems, transplantations of cultivated corneal limbal epithelial cells have recently been reported [26–31]. In such tissue engineering approaches, development of new, effective methods for rapid identification and enrichment of corneal epithelial stem cells would be a considerable advantage since long-term, functional recovery of corneal epithelium is linked to graft constructs that retain viable stem cell populations [26,28,32].

In this study, we examined whether human limbal epithelium contains cells with SP phenotype, similar to stem cells in other organs [6,10–16]. Hoechst 33342 dye exclusion assays revealed that a number of SP cells are present in the limbal epithelium but not in the corneal epithelium (Fig. 1). The mean percentage of SP cells in limbal epithelial cells obtained from six independent experiments was calculated to be 0.29% (data not shown). This is a reasonable abundance value compared with that previously reported in other organs [6,10–16]. Though verapamil is generally used to identify the SP phenotype in the Hoechst 33342 dye exclusion assay, it is insufficient in specificity to demonstrate the contribution of ABCG2 to the SP phenotype of limbal epithelial cells. As ABCG2-specific inhibitors, fumitremorgin C [33], 5D3 monoclonal antibody

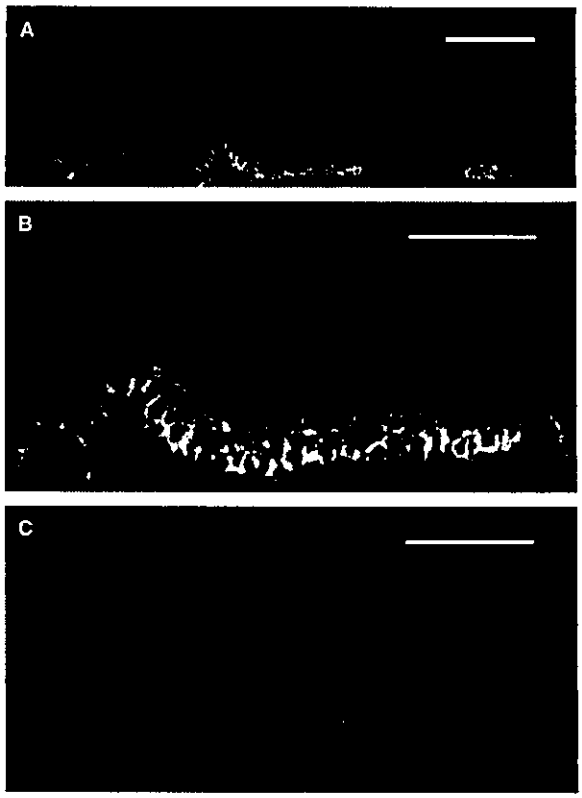

Fig. 4. Expression patterns of the ABCG2 marker using immunomarkers. Distribution of cells expressing ABCG2 protein was examined by immunofluorescence staining using the BXP-21 monoclonal antibody. (A) The basal layer of the limbal epithelium was inconsistently and discontinuously stained with anti-ABCG2 antibody (green). (B) A higher-magnification view of the limbal region showed that positively stained cells are present not only in the basal but also in the suprabasal cells. (C) ABCG2 was not expressed in the corneal epithelium. Nuclei were labeled with propidium iodide (red). Scale bar: 100 μm (A), 50 μm (B, C).

[13,22], and TPS-A [23] are reported. Our SP analysis of limbal epithelial cells using 5D3 and TPS-A showed that both 5D3 and TPS-A effectively inhibit Hoechst 33342 dye efflux from these cells (Fig. 2A, B). These data strongly suggest a correlation between SP phenotype and ABCG2 expression, but the possibility of partial contribution of other transporters to SP phenotype cannot be excluded. Real-time quantitative RT-PCR analysis showed a strong correlation between ABCG2 expression and the SP phenotype. The ABCG2 mRNA expression indices in SP and non-SP cells varied considerably between samples, but SP cells consistently expressed a significantly higher level of ABCG2 mRNA over non-SP cells (Fig. 3B). The variation observed in these experiments may be due to variable conditions of eye bank tissue samples affected by many uncontrolled factors including donor age, death-to-preservation time and tissue storage time.

Immunofluorescence work revealed that ABCG2 was inconsistently expressed within the basal layer of the limbal epithelium (Fig. 4A), but not in the corneal epithelium (Fig. 4C). These observations also indicated that ABCG2 positive cells are present not only in the basal but also in the suprabasal cells in some areas (Fig. 4B). This localization pattern for ABCG2-positive cells coincides almost identically with that for corneal epithelial stem cells demonstrated previously by several investigators [1,2,34–37]. These findings imply that ABCG2 positive cells in the limbal epithelium are putative corneal epithelial stem cells, consistent with the observation that SP cells are present in the limbal epithelium but not in the corneal epithelium (Fig. 1). Flow cytometry revealed that SP cells are only 0.20% of total limbal epithelial cells (Fig. 1A), but immunofluorescence showed that many more cells express ABCG2 (Fig. 4A, B). Because limbal epithelial basal cells have a small cytoplasmic volume, it is not clear whether ABCG2 molecules localize in the plasma membrane or in the cytoplasm (Fig. 4A, B). Since it has been reported that active ABCG2 is expressed on the surface of SP cells, and cytoplasmic ABCG2 cannot efflux Hoechst 33342 dye outside these cells [19,21,38,39], the smaller number of SP cells observed here can be explained by possible cytoplasmic localization of ABCG2. In addition, it is possible that our methods actually underestimate functional SP populations in limbal epithelial cells: cells were collected from eye bank eyes with varying death-to-preservation times and storage conditions, with the likelihood that viability, including dye efflux capability, might be reduced.

One possible biological function of ABCG2 expressed in the limbal epithelium is a protective function. Because Bcrp1/ABCG2 is known to transport a variety of toxic lipophilic compounds [40–42], ABCG2 may protect corneal epithelial stem cells from cytotoxic agents. Recently, Jonker et al. [43] found that Bcrp1/ABCG2-null mice become extremely sensitive to the dietary chlorophyll-breakdown product, pheophorbide a, resulting in severe, sometimes lethal, phototoxic lesions on light-exposed skin. This finding suggests that ABCG2 may protect corneal epithelial stem cells from solar damage. This is also consistent with the assertion that corneal epithelial stem cells are protected from solar damage by melanin pigmentation of the limbus in non-Caucasian people [2]. Another possibility is that ABCG2 may regulate the development of corneal epithelial stem cells by functioning as transporters of small hydrophobic regulatory molecules involved in proliferation, differentiation, or apoptotic pathways. However, the function of ABCG2 expressed in limbal epithelial basal cells remains a subject for further investigations.

In summary, our results suggest that the SP cell phenotype and cellular surface expression of ABCG2 may characterize putative corneal epithelial stem cells. Thus, ABCG2 may serve as a useful cell surface marker in the enrichment of viable corneal epithelial stem cells, and could be readily exploited for new tissue engineering approaches that attempt to reconstruct damaged ocular surfaces using cell transplantation methods.

Acknowledgements: We appreciate useful comments and technical criticism from Prof. D.W. Grainger (Colorado State University, USA) and Dr. A.J. Quantock (Cardiff University, UK). Dr. H. Osada (RIKEN Institute, Japan) provided TPS-A. The present work was supported in part by Grant-in Aid for Scientific Research (15390530) from the Ministry of Education, Culture, Sports, Science and Technology, Japan.

References

[1] Schermer, A., Galvin, S. and Sun, T.T. (1986) J. Cell Biol. 103, 49–62.
[2] Cotsarelis, G., Cheng, S.Z., Dong, G., Sun, T.T. and Lavker, R.M. (1989) Cell 57, 201–209.

[3] Kinoshita, S., Friend, J. and Thoft, R.A. (1981) Invest. Ophthalmol. Vis. Sci. 21, 434–441.
[4] Thoft, R.A. and Friend, J. (1983) Invest. Ophthalmol. Vis. Sci. 24, 1442–1443.
[5] Buck, R.C. (1985) Invest. Ophthalmol. Vis. Sci. 26, 1296–1299.
[6] Goodell, M.A., Brose, K., Paradis, G., Conner, A.S. and Mulligan, R.C. (1996) J. Exp. Med. 183, 1797–1806.
[7] Goodell, M.A., Rosenzweig, M., Kim, H., Marks, D.F., DeMaria, M., Paradis, G., Grupp, S.A., Sieff, C.A., Mulligan, R.C. and Johnson, R.P. (1997) Nat. Med. 3, 1337–1345.
[8] Storms, R.W., Goodell, M.A., Fisher, A., Mulligan, R.C. and Smith, C. (2000) Blood 96, 2125–2133.
[9] Uchida, N., Leung, F.Y. and Eaves, C.J. (2002) Exp. Hematol. 30, 862–869.
[10] Bhattacharya, S., Jackson, J.D., Das, A.V., Thoreson, W.B., Kuszynski, C., James, J., Joshi, S. and Ahmad, I. (2003) Invest. Ophthalmol. Vis. Sci. 44, 2764–2773.
[11] Jackson, K.A., Mi, T. and Goodell, M.A. (1999) Proc. Natl. Acad. Sci. USA 96, 14482–14486.
[12] Hulspas, R. and Quesenberry, P.J. (2000) Cytometry 40, 245–250.
[13] Zhou, S., Schuetz, J.D., Bunting, K.D., Colapietro, A.M., Sampath, J., Morris, J.J., Lagutina, I., Grosveld, G.C., Osawa, M., Nakauchi, H. and Sorrentino, B.P. (2001) Nat. Med. 7, 1028–1034.
[14] Asakura, A. and Rudnicki, M.A. (2002) Exp. Hematol. 30, 1339–1345.
[15] Lechner, A., Leech, C.A., Abraham, E.J., Nolan, A.L. and Habener, J.F. (2002) Biochem. Biophys. Res. Commun. 293, 670–674.
[16] Alvi, A.J., Clayton, H., Joshi, C., Enver, T., Ashworth, A., Vivanco, M.M., Dale, T.C. and Smalley, M.J. (2003) Breast Cancer Res. 5, R1–R8.
[17] Zhou, S., Morris, J.J., Barnes, Y., Lan, L., Schuetz, J.D. and Sorrentino, B.P. (2002) Proc. Natl. Acad. Sci. USA 99, 12339–12344.
[18] Kim, M., Turnquist, H., Jackson, J., Sgagias, M., Yan, Y., Gong, M., Dean, M., Sharp, J.G. and Cowan, K. (2002) Clin. Cancer Res. 8, 22–28.
[19] Scharenberg, C.W., Harkey, M.A. and Torok-Storb, B. (2002) Blood 99, 507–512.
[20] Shimano, K., Satake, M., Okaya, A., Kitanaka, J., Kitanaka, N., Takemura, M., Sakagami, M., Terada, N. and Tsujimura, T. (2003) Am. J. Pathol. 163, 3–9.
[21] Mogi, M., Yang, J., Lambert, J.F., Colvin, G.A., Shiojima, I., Skurk, C., Summer, R., Fine, A., Quesenberry, P.J. and Walsh, K. (2003) J. Biol. Chem. 278, 39068–39075.
[22] Abbott, B.L., Colapietro, A.M., Barnes, Y., Marini, F., Andreeff, M. and Sorrentino, B.P. (2002) Blood 100, 4594–4601.
[23] Woehlecke, H., Osada, H., Herrmann, A. and Lage, H. (2003) Int. J. Cancer 107, 721–728.
[24] Kenyon, K.R. and Tseng, S.C. (1989) Ophthalmology 96, 709–723.
[25] Tsubota, K., Satake, Y., Kaido, M., Shinozaki, N., Shimmura, S., Bissen-Miyajima, H. and Shimazaki, J. (1999) N. Engl. J. Med. 340, 1697–1703.
[26] Pellegrini, G., Traverso, C.E., Franzi, A.T., Zingirian, M., Cancedda, R. and De Luca, M. (1997) Lancet 349, 990–993.
[27] Tsai, R.J., Li, L.M. and Chen, J.K. (2000) N. Engl. J. Med. 343, 86–93.
[28] Rama, P., Bonini, S., Lambiase, A., Golisano, O., Paterna, P., De Luca, M. and Pellegrini, G. (2001) Transplantation 72, 1478–1485.
[29] Tseng, S.C., Meller, D., Anderson, D.F., Touhami, A., Pires, R.T., Gruterich, M., Solomon, A., Espana, E., Sandoval, H., Ti, S.E. and Goto, E. (2002) Adv. Exp. Med. Biol. 506, 1323–1334.
[30] Nishida, K. (2003) Cornea 22, S28–S34.
[31] Nishida, K., Yamato, M., Hayashida, Y., Watanabe, K., Maeda, N., Watanabe, H., Yamamoto, K., Nagai, S., Kikuchi, A., Tano, Y. and Okano, T. (2004) Transplantation 77, 379–385.
[32] Ti, S.E., Anderson, D., Touhami, A., Kim, C. and Tseng, S.C. (2002) Invest. Ophthalmol. Vis. Sci. 43, 2584–2592.
[33] Allen, J.D., van Loevezijn, A., Lakhai, J.M., van der Valk, M., van Tellingen, O., Reid, G., Schellens, J.H., Koomen, G.J. and Schinkel, A.H. (2002) Mol. Cancer Ther. 1, 417–425.
[34] Kurpakus, M.A., Stock, E.L. and Jones, J.C. (1990) Invest. Ophthalmol. Vis. Sci. 31, 448–456.
[35] Matic, M., Petrov, I.N., Chen, S., Wang, C., Dimitrijevich, S.D. and Wolosin, J.M. (1997) Differentiation 61, 251–260.
[36] Pellegrini, G., Dellambra, E., Golisano, O., Martinelli, E., Fantozzi, I., Bondanza, S., Ponzin, D., McKeon, F. and De Luca, M. (2001) Proc. Natl. Acad. Sci. USA 98, 3156–3161.
[37] Espana, E.M., Romano, A.C., Kawakita, T., Di Pascuale, M., Smiddy, R. and Tseng, S.C. (2003) Invest. Ophthalmol. Vis. Sci. 44, 4275–4281.
[38] Rocchi, E., Khodjakov, A., Volk, E.L., Yang, C.H., Litman, T., Bates, S.E. and Schneider, E. (2000) Biochem. Biophys. Res. Commun. 271, 42–46.
[39] Summer, R., Kotton, D.N., Sun, X., Ma, B., Fitzsimmons, K. and Fine, A. (2003) Am. J. Physiol. Lung. Cell. Mol. Physiol. 285, L97–L104.
[40] Allen, J.D., Brinkhuis, R.F., Wijnholds, J. and Schinkel, A.H. (1999) Cancer Res. 59, 4237–4241.
[41] Jonker, J.W., Smit, J.W., Brinkhuis, R.F., Maliepaard, M., Beijnen, J.H., Schellens, J.H. and Schinkel, A.H. (2000) J. Natl. Cancer Inst. 92, 1651–1656.
[42] Robey, R.W., Medina-Perez, W.Y., Nishiyama, K., Lahusen, T., Miyake, K., Litman, T., Senderowicz, A.M., Ross, D.D. and Bates, S.E. (2001) Clin. Cancer Res. 7, 145–152.
[43] Jonker, J.W., Buitelaar, M., Wagenaar, E., Van Der Valk, M.A., Scheffer, G.L., Scheper, R.J., Plosch, T., Kuipers, F., Elferink, R.P., Rosing, H., Beijnen, J.H. and Schinkel, A.H. (2002) Proc. Natl. Acad. Sci. USA 99, 15649–15654.

TISSUE ENGINEERING
Volume 10, Number 7/8, 2004

Immobilization of Cell-Adhesive Peptides to Temperature-Responsive Surfaces Facilitates Both Serum-Free Cell Adhesion and Noninvasive Cell Harvest

MITSUHIRO EBARA,[1] MASAYUKI YAMATO, Ph.D.,[2] TAKAO AOYAGI, Ph.D.,[2] AKIHIKO KIKUCHI, Ph.D.,[2] KIYOTAKA SAKAI, Ph.D.,[1] and TERUO OKANO, Ph.D.[2]

ABSTRACT

We have developed temperature-responsive cell culture surfaces to harvest intact cell sheets for tissue-engineering applications. Both cost and safety issues (e.g., prions, bovine spongiform encephalopathy) are compelling reasons to avoid use of animal-derived materials, including serum, in such culture. In the present study, synthetic cell-adhesive peptides are immobilized onto temperature-responsive polymer-grafted surfaces, and cell adhesion and detachment under serum-free conditions were examined. The temperature-responsive polymer poly(*N*-isopropylacrylamide) (PIPAAm) was functionalized by copolymerization with a reactive comonomer having both a carboxyl group and an isopropylacrylamide group. These copolymers were covalently grafted onto tissue culture-grade polystyrene dishes. Synthetic cell-adhesive peptides were then immobilized onto these surfaces via carboxyl groups. Bovine aortic endothelial cells both adhered and spread on these surfaces even under serum-free conditions at 37°C, similar to those in 10% serum-supplemented culture. Spread cells promptly detached from the surfaces on lowering culture temperatures below the lower critical solution temperature of the polymer, 32°C. These surfaces would be useful for serum-free culture for tissue-engineering applications.

INTRODUCTION

WE HAVE DEVELOPED temperature-responsive culture dishes on which various cell types adhere and multiply similarly to cells on tissue culture polystyrene (TCPS) dishes at 37°C. On these surfaces, spread cells spontaneously detach on reduction of the culture temperature below the polymer's lower critical solution temperature (LCST, 32°C), as a result of rapid hydration of the grafted dish polymer surface.[1,2] When the culture temperature is reduced after cells reach confluency, all cells are harvested as a single contiguous cell sheet.[3,4] These transplantable cell sheets retain cell–cell junctional proteins as well as intact extracellular matrix underneath the cell sheets.[3,5,6] Furthermore, cell function is often maintained: harvested pulsating cardiac myocyte sheets become stratified *in vitro*,[7] and can be grafted *in vivo*.[8] Histological and functional integration of cardiac myocyte sheets is shown after culture stratification and tissue grafting. Therefore, we currently utilize the culture method for tissue-engineering applications.

Both cost and safety issues in cell culture argue for the development of cell culturing, harvesting, and device construction methods that require no mammalian-sourced

[1]Department of Applied Chemistry, Waseda University, Tokyo, Japan.
[2]Institute of Advanced Biomedical Engineering and Science, Tokyo Women's Medical University, Tokyo, Japan.

components. For example, cell culture reagents are often sourced from bovine serum at considerable expense, and the risk of cross-infecting humans with bovine pathogens (viruses, prions, and spongiform encephalopathy in Europe and Japan) is a concern.[9,10] Because temperature-responsive culture dishes require cell-adhesive proteins for cell adhesion and spreading, like tissue culture polystyrene (TCPS), serum or cell-adhesive proteins such as fibronectin derived from serum are commonly utilized. To achieve serum-free culture in the present study, the common synthetic cell adhesive peptide Arg-Gly-Asp-Ser (RGDS)[11,12] was immobilized on temperature-responsive culture dishes on which copolymers of *N*-isopropylacrylamide (IPAAm) and 2-carboxyiso-propylacrylamide (CIPAAm)[13] had been covalently grafted. This surface affords adhesion, culture, and harvest of cell sheets under serum-free conditions.

MATERIALS AND METHODS

Materials

N-Isopropylacrylamide (IPAAm) was kindly provided by Kohjin (Tokyo, Japan) and purified by recrystallization from *n*-hexane. 2-Carboxyisopropylacrylamide (CIPAAm) was synthesized as described previously.[13] Acrylic acid (AAc) was purchased from Wako Pure Chemicals (Tokyo, Japan) and distilled under reduced pressure. TCPS dishes (Falcon 3001) were purchased from BD Biosciences Discovery Labware (Oxnard, CA). Synthetic cell-adhesive peptides were purchased from Sigma (St. Louis, MO). 1-Ethyl-3-(3-dimethylaminopropyl)-carbodiimide hydrochloride (water-soluble carbodiimide; WSC) was purchased from Dojindo Laboratories (Kumamoto, Japan). Bovine aortic endothelial cells (BAECs) were provided by

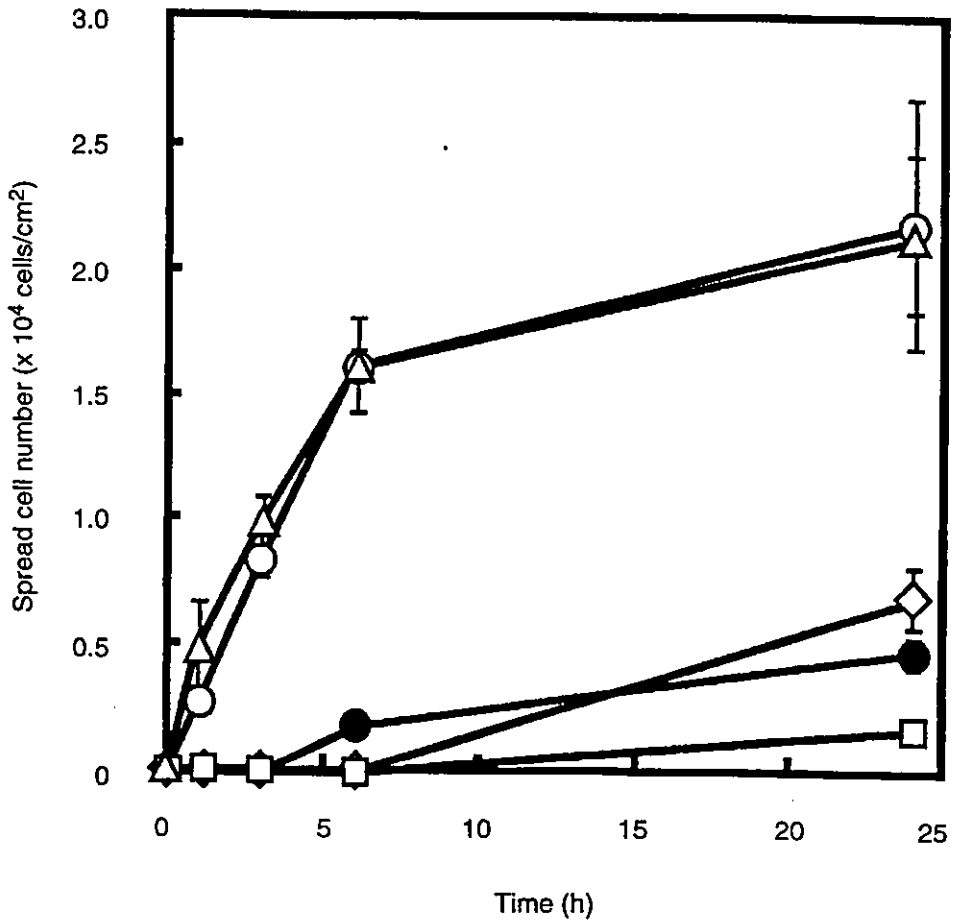

FIG. 1. BAEC spreading on RGDS-immobilized temperature-responsive culture surfaces. RGDS peptides were covalently grafted on P(IPAAm-*co*-CIPAAm)-grafted surfaces (IPAAm: CIPAAm, 99:1 in feed). The feed concentration of RGDS peptides was 0 [RGDS(0)-IC(1), solid circles], 0.2 [RGDS(0.2)-IC(1), open circles], 1 [RGDS(1)-IC(1), triangles], and 2 mM [RGDS(2)-IC(1), squares]. BAEC spreading was examined without serum at 37°C.

the Health Science Research Resources Bank (JCRB 0099; Osaka, Japan). Trypsin–EDTA solution, streptomycin, and penicillin were purchased from GIBCO-BRL (Grand Island, NY). Dulbecco's modified Eagle's medium (DMEM) was purchased from Iwaki (Chiba, Japan). EGM-2 (growth factor supplements) was purchased from Cambrex BioScience Walkersville, (Walkersville, MD).

Grafting of temperature-responsive polymer and RGDS immobilization

Temperature-responsive polymer-grafted surfaces were prepared as described previously.[4,14] Briefly, IPAAm and carboxylic monomer CIPAAm were dissolved in 2-propanol at a total concentration of 55% (w/w) and 30-μL aliquots were spread uniformly over 35-mm TCPS dishes. These solutions contained different concentrations of CIPAAm (1–10 mol%). Then, electron beam irradiation using an area beam electron-processing system (Curetron EBC-200-AA2; Nissin High Voltage, Kyoto, Japan) at a radiation dose of 0.3 MGy promoted polymerization and covalent grafting of copolymer onto TCPS surfaces. After rinsing and drying, 1 mL of Dulbecco's phosphate-buffered saline (PBS; pH 7.4) containing both RGDS peptides (0.2, 1 and 2 mM) and carbodiimide coupling reagent, WSC (the same concentration of peptides), was spread over each surface at room temperature. After 1 day of incubation, these dishes were rinsed with distilled water and sterilized with ethylene oxide after drying. These RGDS-immobilized P(IPAAm-*co*-CIPAAm)-grafted TCPS surfaces were abbreviated as RGDS(X)-IC(Y), where X is the feed RGDS concentration (millimolar) and Y is the mole percentage of carboxyl-containing monomer groups in the feed.

Cell adhesion and spreading assay in culture

BAECs were expanded on TCPS dishes with DMEM supplemented with 10% fetal bovine serum (FBS), penicillin (100 units/mL), and streptomycin (100 μg/mL) at 37°C in a humidified atmosphere with 5% CO2. BAECs were harvested from TCPS dishes with 0.25% trypsin–0.26 mM EDTA in PBS. DMEM without serum was added, and the cells were centrifuged and resuspended in DMEM without serum. A fixed number of cells (2×10^4 cells/cm^2) was plated onto peptide-immobilized surfaces and cultured at 37 or 20°C. Cell morphology was monitored and photographed under a phase-contrast microscope (TE300; Nikon, Tokyo, Japan) at various times. The cell number was also counted on printed photographs and averaged ($n = 3$). The spread area of individual cells on each surface was determined by tracing the outline of each cell and integrating this area with NIH Image (version 1.62) software for the Macintosh. Spread cell number and cell area are presented as means ± standard deviation ($n = 3$).

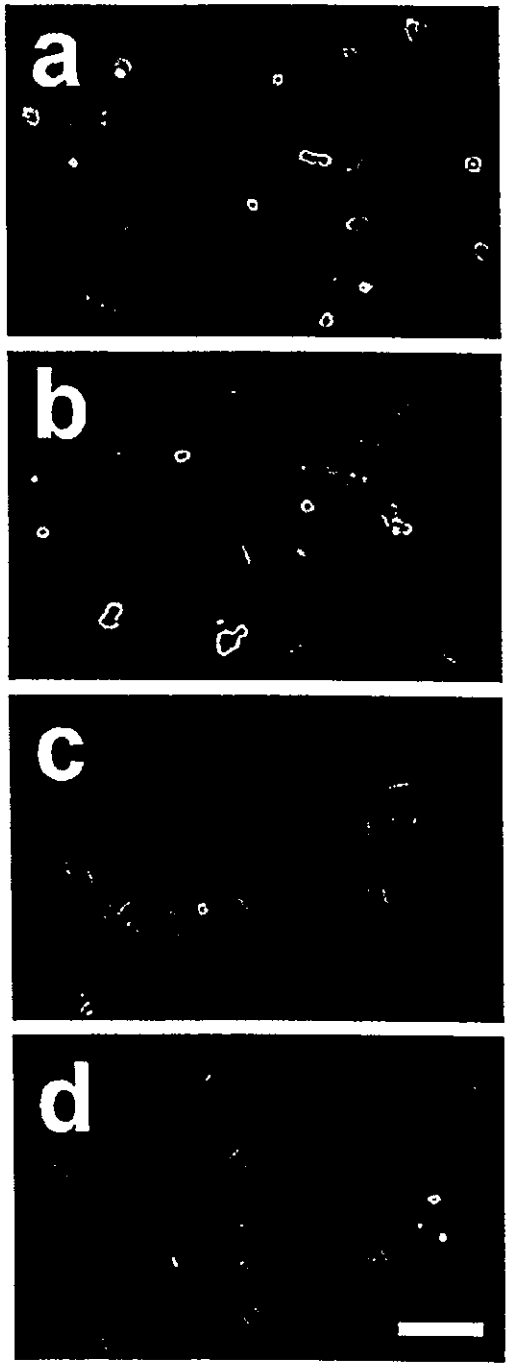

FIG. 2. Phase-contrast photographs of BAECs on RGDS-immobilized temperature-responsive culture surfaces. Representative cell morphologies after 24 h of culture without serum at 37°C are shown. (a) RGDS(0)-IC(1); (b) RGDS(0.2)-IC(1); (c) RGDS(1)-IC(1); (d) RGDS(2)-IC(1). Scale bar: 100 μm.

Cell detachment assay

Cell detachment from peptide-immobilized surfaces, done by reducing the cell culture temperature, was examined. BAECs were seeded sparsely (2.0×10^4 cells/cm^2) and densely (2.0×10^5 cells/cm^2) for the single-cell detachment assay and cell sheet detachment assay, respectively. For the single-cell detachment assay, BAECs were cultured for 24 h at 37°C. Culture medium was serum-free DMEM supplemented only with antibiotics. For the cell sheet detachment assay, BAECs were cultured for 1 week at 37°C. Culture medium was serum-free DMEM supplemented with antibiotics and EGM-2 containing human fibroblast growth factor B (hFGF-B), vascular endothelial growth factor (VEGF), recombinant insulin-like growth factor I (LongR^{3}IGF-I; Cell Sciences, Canton, MA), ascorbic acid, heparin, human epidermal growth factor (hEGF), hydrocortisone, gentamicin/amphotericin B (GA-1000) and lacking FBS. Dishes were then transferred to a CO_2 incubator equipped with a cooling unit fixed at 20°C to induce detachment by polymer surface swelling. Photomicrographs were taken at various times. The spread cell number was presented as means ± standard deviation ($n = 3$).

RESULTS

Cell adhesion on RGDS-immobilized temperature-responsive culture surfaces

Cell spreading was examined on synthetic cell-adhesive RGDS-immobilized surfaces under serum-free conditions. Increasing the peptide feed amounts increased cell spreading significantly in a dose-dependent manner (Fig. 1). Even on surfaces without immobilized peptides, scarce cell spreading was observed after 24 h of culture at 37°C, and this seemed to result from cell-secreted cell adhesion molecules. When the PIPAAm-grafted surfaces lacking carboxyl groups were subjected to similar blank peptide immobilization reactions with cell-adhesive pep-

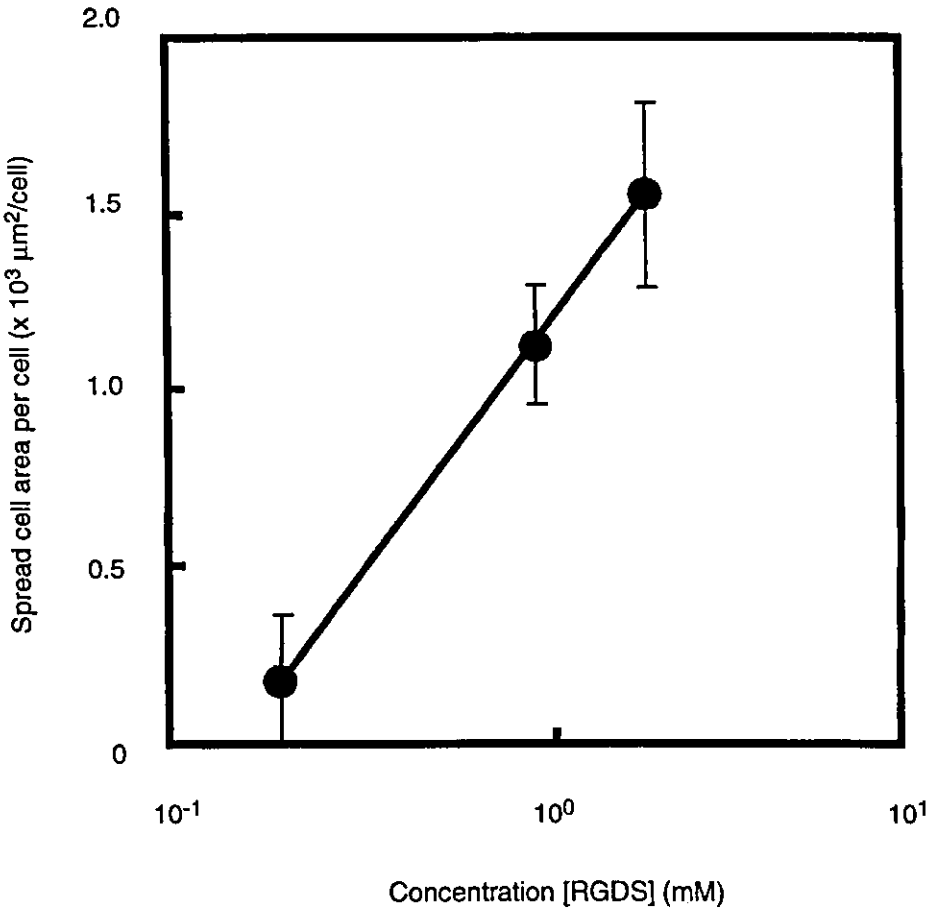

FIG. 3. Spread areas of individual BAECs on RGDS-immobilized temperature-responsive culture surfaces. Cell area on RGDS(0.2)-IC(1), RGDS(1)-IC(1), and RGDS(2)-IC(1) was measured after 24 h of culture without serum at 37°C, and plotted against the feed concentration of RGDS peptides.

tides, a similar basal level of cell spreading was observed in serum-free medium (data not shown). The total area of each cell was evaluated (Figs. 2 and 3). BAECs exhibited less spreading on surfaces immobilized with lesser amounts of cell-adhesive peptides. By increasing the peptide density, cells exhibited highly spread morphologies. Interestingly, cell spreading enhancement correlated well with the logarithm of the feed amount of cell-adhesive peptides (Fig. 3).

BAEC spreading was also examined on surfaces having various feed compositions of carboxyl comonomer groups, RGDS(2)-IC(*Y*), with a fixed (2 mM) feed of cell-adhesive peptide (Fig. 4). With increasing CIPAAm amounts, the spread cell number increased. Under optimized conditions of cell-adhesive peptide immobilization, RGDS(2)-IC(1), BAEC spreading in serum-free culture was the same as that observed on RGDS(0)-IC(1) in 10% FBS-supplemented DMEM (Fig. 5). On the other hand, BAEC spreading improvement was insignificant on a grafted RGDS(2)-IA(1) surface containing another comonomer, AAc, in place of CIPAAm under identical conditions. Cell spreading on RGDS(2)-IA(1) after 24 h of serum-free culture at 37°C was ~33% of that on RGDS(2)-IC(1). To confirm that the observed enhancement of cell attachment is mediated by immobilized RGDS peptides, competition assays were performed (Fig. 5). BAECs were suspended in serum-free DMEM containing RGDS peptides (50 μM) and incubated for 15 min at 37°C. These cells were then plated onto RGDS(*X*)-IC(1) and incubated at 37°C under serum-free conditions. Preincubation with soluble synthetic cell-adhesive peptides resulted in diminished cell spreading because RGDS peptides occupied cell membrane integrin, extracellular matrix receptors during the preincubation. Cell spreading was also considerably reduced when cells were seeded onto these surfaces at 20°C below the surface LCST.

Addition of growth factor supplements and high-density cell seeding allow cells to grow and reach confluency on RGDS(2)-IC(1) without serum (Fig. 6). RGDS

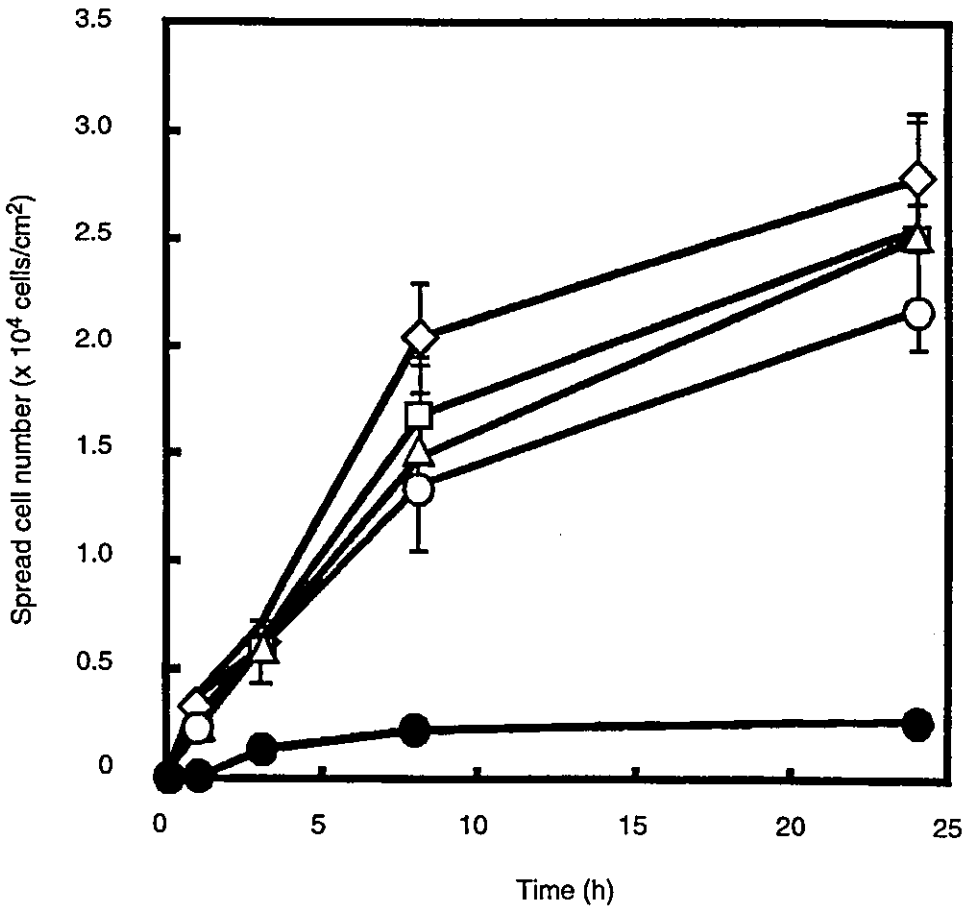

FIG. 4. BAEC spreading on RGDS-immobilized surfaces with various feed concentrations of CIPAAm comonomer. Temperature-responsive culture surfaces were prepared with various feed ratios of CIPAAm. RGDS peptides were then covalently grafted onto the surfaces. Feed concentrations of CIPAAm were 0 (solid circles), 1 (open circles), 3 (triangles), 5 (squares), and 10 mol% (diamonds). BAEC spreading was examined without serum at 37°C.

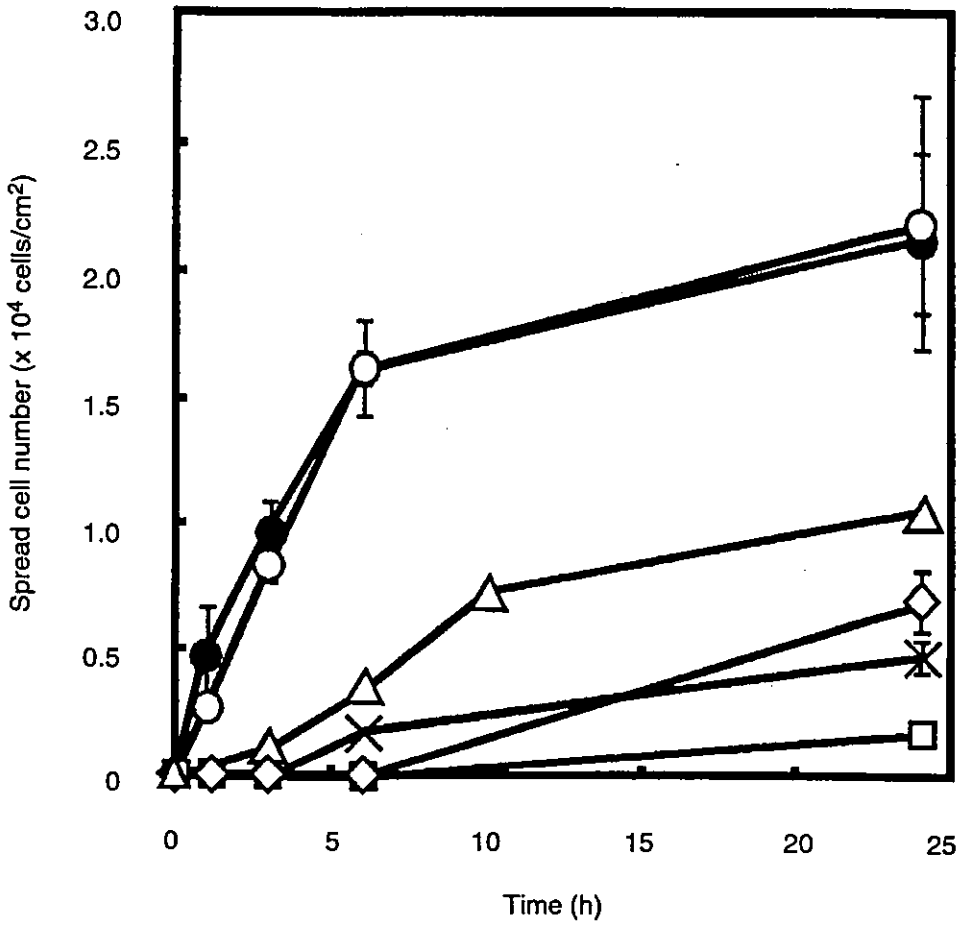

FIG. 5. Competitive assay for BAEC spreading on RGDS-immobilized temperature-responsive surfaces [RGDS(0)-IC(1), mults]). Immobilization of RGDS peptides [RGDS(2)-IC(1), open circles] achieves improvement of BAEC spreading equal to that on 10% FBS supplemented DMEM (solid circles). BAEC spreading on RGDS(2)-IA(1) was suppressed (triangles). BAEC spreading on RGDS(2)-IC(1) was inhibited by preincubation with soluble RGDS peptides (diamonds) and also suppressed at 20°C below the LCST (squares).

immobilization promotes quick cell attachment and growth confluency compared with surfaces before immobilization.

Single-cell and cell sheet detachment by lowering culture temperature

BAECs were challenged to detach from cell-adhesive RGDS-immobilized culture surfaces by reducing the temperature before and after reaching confluency (Figs. 7 and 8). Simply by reducing the culture temperature, single BAECs were spontaneously detached from these surfaces, changing their shapes from spread to round cell morphologies. But the detachment rate was decreased with increasing feed amounts of cell-adhesive peptides (Fig. 7). All spread BAECs were detached from surfaces grafted with less than 5 mol% CIPAAm and 2 mM cell-adhesive peptides. In contrast, few cells detached from the RGDS(2)-IC(10) surface with a high density of immobilized peptides. When the culture temperature was reduced after BAECs reached confluency in growth factor-supplemented serum-free culture, all cells spontaneously detached as a single contiguous cell sheet (Fig. 8), similar to many results we reported previously with pure PIPAAm culture surfaces with serum-containing medium.[1-8]

DISCUSSION

We have previously reported that 5 and 10 mol% feed of CIPAAm comonomer with PIPAAm results in 4.8 and 8.8 mol% incorporation in the linear polymerization in solution.[13] If a similar reaction occurs on the surface, carboxyl groups are introduced onto the temperature-re-

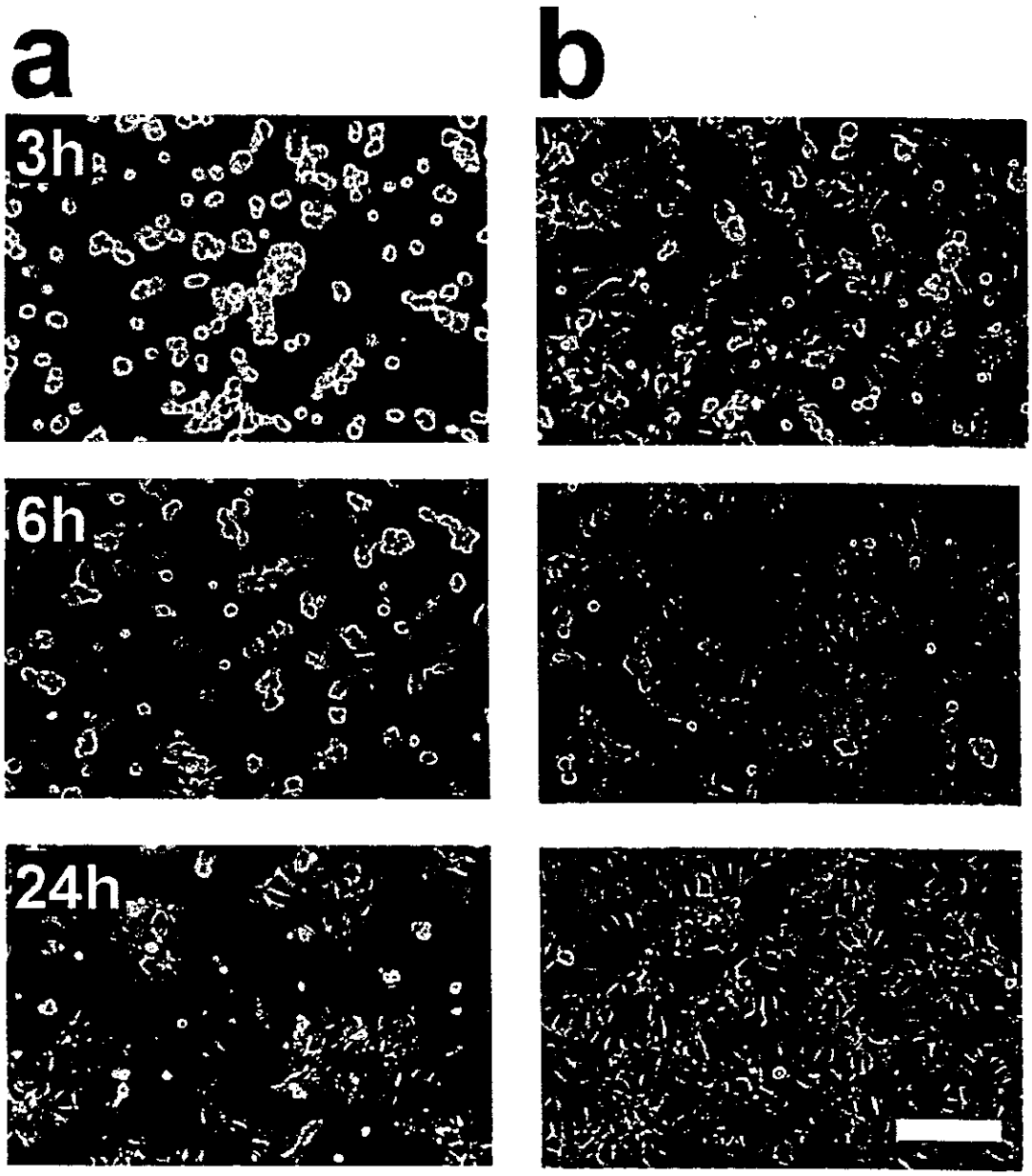

FIG. 6. Phase-contrast photographs of BAEC growth behavior on P(IPAAm-*co*-CIPAAm)-grafted TCPS surfaces before and after RGDS immobilization. Representative cell morphologies after various times in culture with several growth factor supplements at 37°C are shown. (a) IC(1); (b) RGDS(2)-IC(1). Scale bar: 100 μm.

sponsive surface at approximate at densities of 0.2, 0.6, 1.0, and 2.0 nmol/cm^2 for RGDS(X)-IC(1), -IC(3), -IC(5), and -IC(10) surfaces, respectively. These values were calculated on the basis of grafted polymer amounts on surfaces (approximately 2 μg/cm^2) determined by attenuated total reflection Fourier transform infrared (ATR-FTIR) spectra.[14] Actually, cell spreading is increasingly promoted as the carboxyl group density increases on the surface (Fig. 4). However, cell spreading improvement nearly saturates at 1 mol% CIPAAm comonomer in the feed. Feed RGDS concentration also affects BAEC spreading behavior (Fig. 3). Massia and Hubbell reported that the minimal RGD peptide density required for fibroblast spreading was approximately 1 fmol/cm^2.[15] Because cell spreading saturation was observed at a 10^4-fold higher density of carboxyl groups in the present study, only fractional amounts of surface carboxyl groups are reacted and/or only minimal amounts of the surface-immobilized peptides were exposed to cells. Because carbodiimide chemistry was utilized for cell-adhesive peptide immobilization here and the reaction also occurs between the carboxyl terminus of one

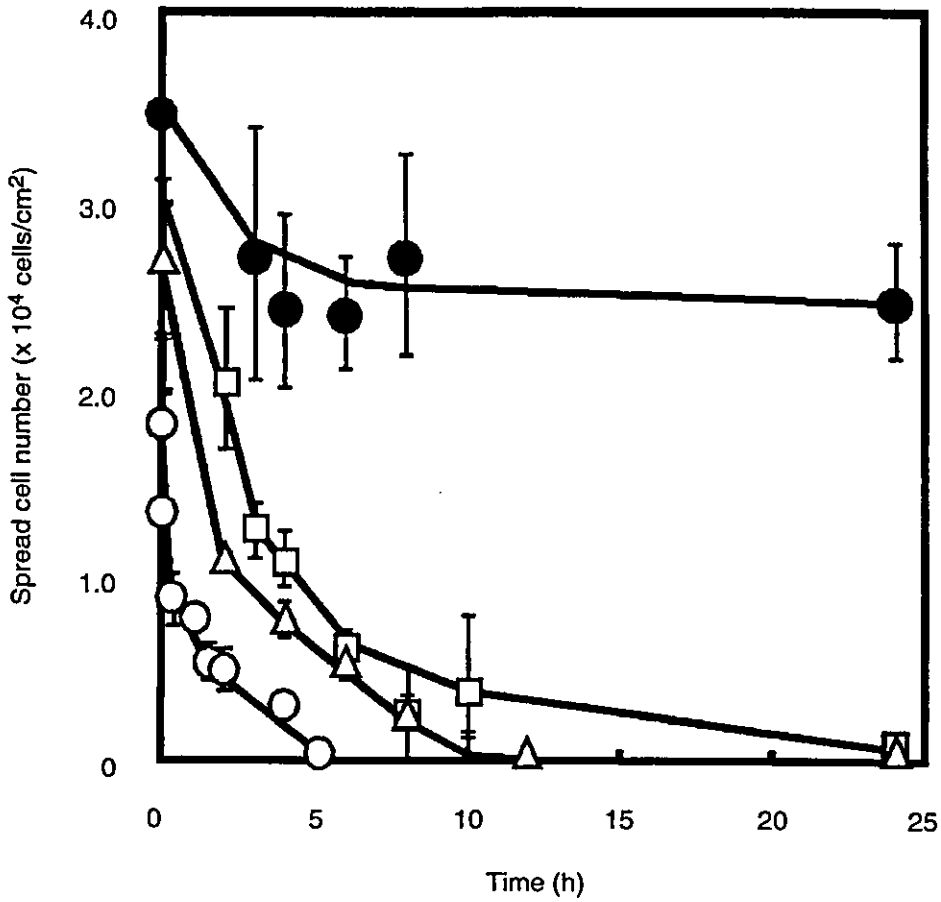

FIG. 7. BAEC detachment from RGDS-immobilized temperature-responsive culture surfaces. RGDS(2)-IC(*X*) surfaces were subjected to low-temperature treatment at 20°C after 24 h of culture at 37°C without serum. CIPAAm compositions: 1 mol% (open circles); 3 mol% (triangles); 5 mol% (squares); and 10 mol% (solid circles).

RGDS peptide and the amino terminus of another RGDS, several synthetic peptides could be linked in tandem. This might explain the higher carboxyl group density required for cell surface saturation. The saturation of feed RGDS concentration for BAEC spreading was observed at 1 mM. This is 50 to 100 times higher than the content of introduced grafted carboxyl groups.

BAEC spreading on RGDS(2)-IA(1) was less than that on RGDS(2)-IC(1) in serum-free culture. Because the intended coupling carboxyl group of acrylic acid (AAc) is closer to its backbone vinyl group than to that of CIPAAm, RGDS peptides are thought to react only with difficulty with the carboxyl groups hindered by neighboring bulky isopropyl groups of IPAAm. Moreover, unreacted carboxyl groups of AAc shift the bulk and surface-grafted copolymer LCST above 37°C whereas those of CIPAAm does not.[13, 14] This LCST shift results in hydration of grafted culture surfaces and hampers cell adhesion at 37°C. Even on RGDS(2)-IC(1), cell seeding below the surface LCST resulted in less cell spreading (Fig. 5). It is plausible that the polymer-grafted surface loses its mechanics and becomes softer below the LCST (Fig. 9). In addition, the density of RGDS exposed to cells decreases under this condition because of the hindrance of hydrated polymer surface chains.

We have previously shown that spread cells detach from PIPAAm-grafted surfaces by lowering the temperature to below the LCST.[1] Because deposited cell-adhesive proteins such as fibronectin and laminin also detach together with cells from the surface of dishes, we concluded that enzyme-free cell detachment from temperature-responsive culture dishes may be attributed to reduced interactions between cell-adhesive proteins and hydrated PIPAAm chains below the LCST.[3,5] In the present study, cell adhesive peptides were covalently immobilized instead of cell-adhesive protein adsorption. Therefore, cell detachment requires dissociation of the immobilized ligands from cell surface integrin receptors.

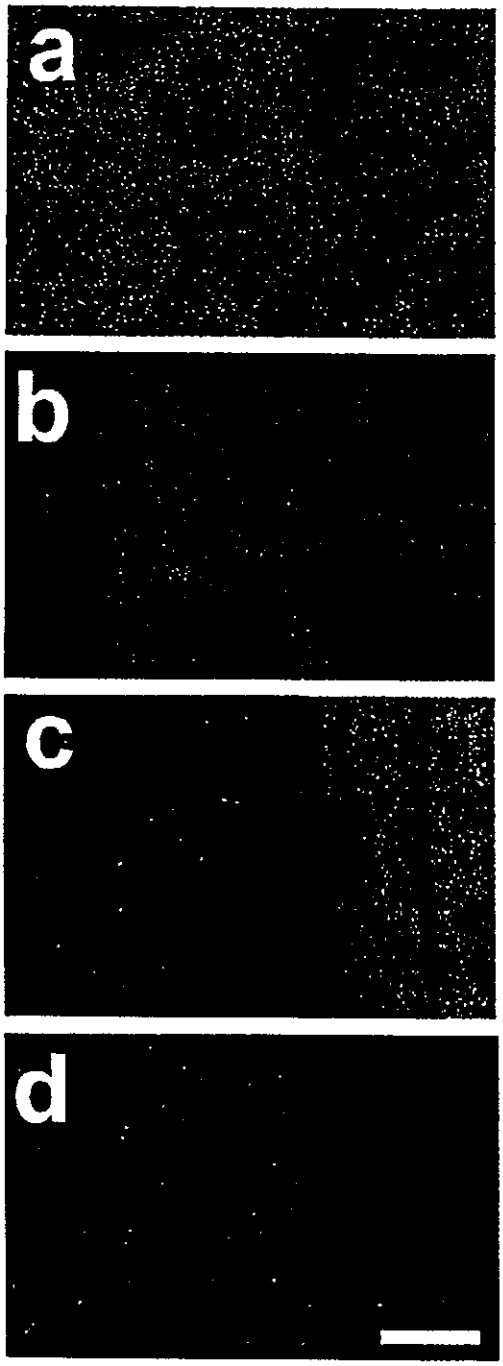

FIG. 8. Harvest of BAEC cultured contiguous sheets from RGDS-immobilized temperature-responsive culture surfaces, RGDS(2)-IC(1), at 20°C below the LCST and under serum-free conditions. (a) 0 min, (b) 60 min, (c) 70 min, and (d) 90 min after reducing culture temperature. Scale bar: 500 μm.

This seems to be a major reason for the retarded cell detachment kinetics compared with that on PIPAAm-grafted surfaces in 10% FBS-supplemented medium.[14] Cell detachment rates in serum-free media decreased with temperature reductions, dependent on immobilized RGDS numbers (Fig. 7). In the case of RGDS-immobilized surfaces containing 10 mol% CIPAAm, RGD(2)-IC(10), 70% of the cultured cells remained spread after 24 h of incubation at 20°C (below the LCST). By contrast, almost all cells detached from RGDS-immobilized surfaces containing less than 5 mol% CIPAAm under these conditions. Interestingly, no significant differences were observed between cells on RGDS(2)-IC(5) and -IC(10) for cell spreading, whereas cell detachment after reducing the temperature was significantly hampered on RGDS(2)-IC(10) in serum-free media. As seen in Figs. 6 and 8, cells would also be recovered as a contiguous monolayer sheet by applying a combination of growth factor supplements.

The main mechanism of cell detachment may involve changes in both polymer-grafted surface rigidity and apparent RGDS density exposed to cells, induced by lowering the temperature. It has been widely reported that cells prefer a stiff substrate to a soft one for their adhesion and downstream cell adhesion events.[16,17] In particular, cells on gradient-compliant hydrogels are likely to move from the soft region toward the stiff region.[18] Mrksich and co-workers also developed a cell detachment system based on an electroactive self-assembled monolayer, and this substrate can selectively detach cells from the surface by releasing ligands.[19] In contrast to their system, our RGDS-immobilized temperature-responsive surface can detach cells from the surface by controlling the binding affinity between ligands and receptors, with RGDS remaining on the cell culture surface.

By introducing synthetic cell-adhesive peptides onto temperature-responsive culture surfaces, both serum-free cell adhesion and noninvasive cell harvest were achieved. Cell proliferation was promoted with growth factors prepared by recombinant technology. By combining the present culture dishes with recombinant growth factors, animal-derived materials can be completely excluded from culture. These techniques would be useful for tissue engineering and other biotechnology applications.

ACKNOWLEDGMENTS

We appreciate the continued useful comments and technical criticisms from Prof. D.W. Grainger (Colorado State University, Fort Collins, CO). This work is supported in part by Grants-in-Aid for Scientific Research by the Ministry of Education, Culture, Sports, Science, and Technology of Japan. The present study is supported in part by the Japanese Ministry for Culture, Sports, Education, Science, and Technology, Core Research for Evolutional Science and Technology (CREST).

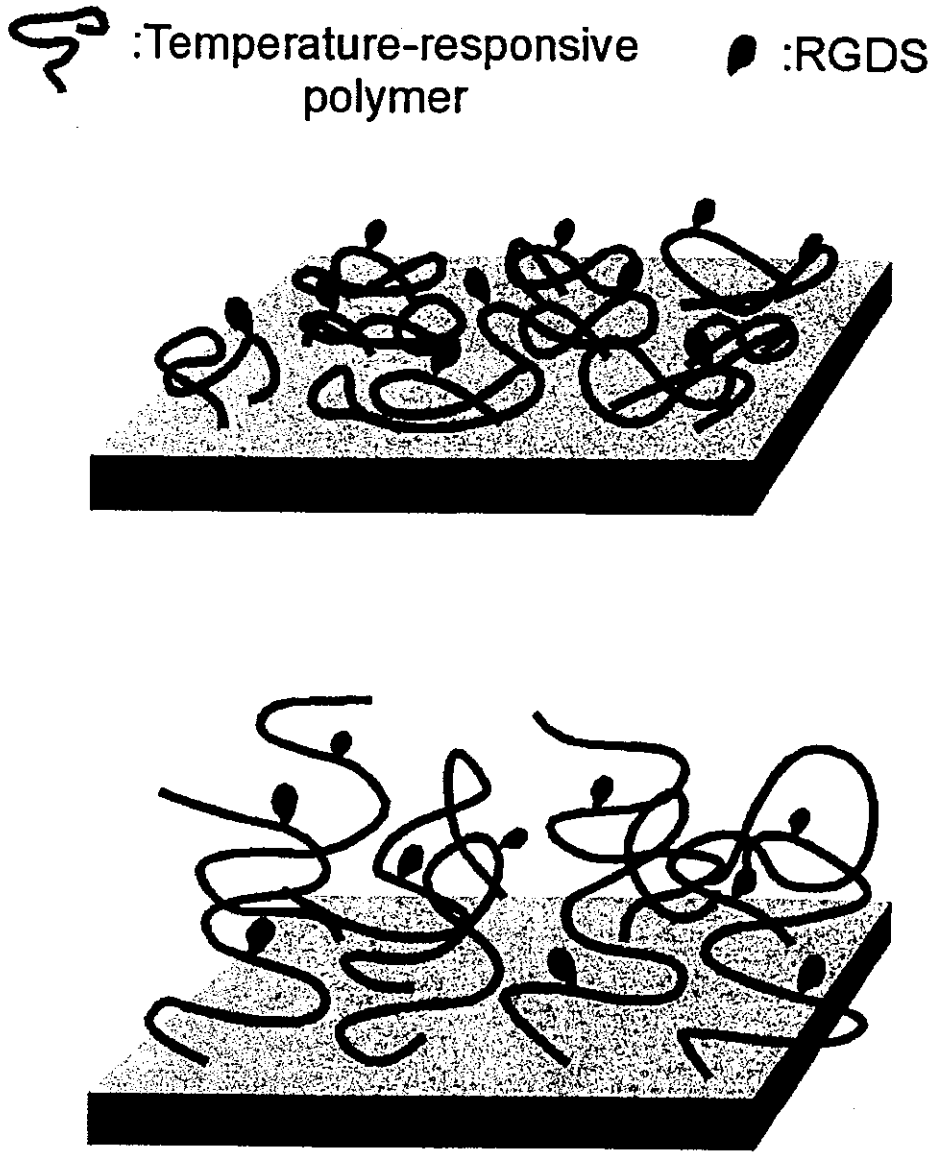

FIG. 9. Schematic illustration of mechanism for serum-free temperature dependence of RGDS-immobilized temperature-responsive surfaces. RGDS peptides were exposed at 37°C (*top*), but were hindered by hydrated polymer chains below the LCST (*bottom*).

REFERENCES

1. Yamada, N., Okano, T., Sakai, H., Karikusa, F., Sawasaki, Y., and Sakurai, Y. Thermoresponsive polymeric surfaces: Control of attachment and detachment of cultured cells. Macromol. Chem. Rapid Commun. **11**, 571, 1990.
2. Yamato, M., Okuhara, M., Karikusa, F., Kikuchi, A., Sakurai, Y., and Okano, T. Signal transduction and cytoskeletal reorganization are required for cell detachment from cell culture surfaces grafted with a temperature-responsive polymer. J. Biomed. Mater. Res. **44**, 44, 1999.
3. Kushida, A., Yamato, M., Konno, C., Kikuchi, A., Sakurai, Y., and Okano, T. Decrease in culture temperature releases monolayer endothelial cell sheets together with deposited fibronectin matrix form temperature-responsive culture surfaces. J. Biomed. Mater. Res. **45**, 355, 1999.
4. Hirose, M., Kwon, O. H., Yamato, M., Kikuchi, A., and Okano, T. Creation of designed shape cell sheets that are noninvasively harvested and moved onto another surface. Biomacromolecules **1**, 377, 2000.
5. Yamato, M., Utsumi, M, Kushida, A., Konno, C., Kikuchi, A., and Okano, T. Thermoresponsive culture dishes allow the intact harvest of multilayered keratinocyte sheets without dispase by reducing temperature. Tissue Eng. **7**, 473, 2001.
6. Kushida, A., Yamato, M., Konno, C., Kikuchi, A., Sakurai, Y., and Okano, T. Temperature-responsive culture dishes allow nonenzymatic harvest of differentiated Madin-

Darby canine kidney (MDCK) cell sheets. J. Biomed. Mater. Res. **51**, 216, 2000.
7. Shimizu, T., Yamato, M., Akutsu, T., Shibata, T., Isoi, Y., Kikuchi, A., Umezu, M., and Okano, T. Electrically communicating three-dimensional cardiac tissue mimic fabricated by layered cultured cardiomyocyte sheet. J. Biomed. Mater. Res. **60**, 110, 2002.
8. Shimizu, T., Yamato, M., Isoi, Y., Akutsu, T., Setomaru, T., Abe, K., Kikuchi, A., Umezu, M., and Okano, T. Fabrication of pulsatile cardiac tissue grafts using a novel 3-dimensional cell sheet manipulation technique and temperature-responsive cell culture surfaces. Circ. Res. **90**, e40, 2002.
9. Erstad, B.L. Implications of prion-induced diseases for animal-derived pharmaceutical products. Am. J. Health System Pharm. **59**, 254, 2002.
10. Wenz, B., Oesch, B., and Horst, M. Analysis of the risk of transmitting bovine spongiform encephalopathy though bone grafts derived from bovine bone. Biomaterials **22**, 1599, 2001.
11. Piershbacher, M.D., and Rouslahti, E. Variants of the cell recognition site of fibronectin that retain attachment-promoting activity. Proc. Natl. Acad. Sci. U.S.A. **81**, 5985, 1984.
12. Hynes, R.O. Integrins: Versatility, modulation, and signaling in cell adhesion. Cell **69**, 11, 1992.
13. Aoyagi, T., Ebara, M., Sakai, K., Sakurai, Y., and Okano, T. Novel bifunctional polymer with reactivity and temperature sensitivity. J. Biomater. Sci. Polym. Ed. **1**, 101, 2000.
14. Ebara, M., Yamato, M., Hirose, M., Aoyagi, T., Sakai, K., and Okano T. Copolymerization of 2-carboxyisopropylacrylamide with *N*-isopropylacrylamide accelerates cell detachment from grafted surfaces by reducing temperature. Biomacromolecules **4**, 344, 2003.
15. Massia, S.P., and Hubbell, J.A. An RGD spacing of 440 nm is sufficient for integrin $\alpha_v\beta_3$-mediated fibroblast spreading and 140 nm for focal contact and stress fiber formation. J. Cell Biol. **114**, 1089, 1991.
16. Wang, H.-B., Dembo, M., and Wang, Y.-L. Substrate flexibility regulates growth and apoptosis of normal but not transformed cells. Am. J. Physiol. Cell. Physiol. **279**, C1345, 2000.
17. Choquet, D., Felsenfeld, D.P., and Sheetz, M.P. Extracellular matrix rigidity causes strengthening of integrin–cytoskeleton linkages. Cell **88**, 39, 1997.
18. Wong, J.Y., Velasco, A., Rajagopalan, P., and Pham, Q. Directed movement of vascular smooth muscle cells on gradient-compliant hydrogels. Langmuir **19**, 1908, 2003.
19. Yeo, W.-S., Hodneland, C.D., and Mrksich, M. Electroactive monolayer substrates that selectively release adherent cells. Chembiochem **7/8**, 590, 2001.

Address reprint requests to:
Teruo Okano, Ph.D.
Institute of Advanced Biomedical Engineering and Science
Tokyo Women's Medical University
8-1 Kawada-cho, Shinjuku-ku
Tokyo 162-8666, Japan

E-mail: tokano@abmes.twmu.ac.jp

ORIGINAL ARTICLE

Corneal Reconstruction with Tissue-Engineered Cell Sheets Composed of Autologous Oral Mucosal Epithelium

Kohji Nishida, M.D., Ph.D., Masayuki Yamato, Ph.D., Yasutaka Hayashida, M.D., Katsuhiko Watanabe, M.Sc., Kazuaki Yamamoto, M.Sc., Eijiro Adachi, M.D., Ph.D., Shigeru Nagai, M.Sc., Akihiko Kikuchi, Ph.D., Naoyuki Maeda, M.D., Ph.D., Hitoshi Watanabe, M.D., Ph.D., Teruo Okano, Ph.D., and Yasuo Tano, M.D., Ph.D.

ABSTRACT

BACKGROUND

Ocular trauma or disease may lead to severe corneal opacification and, consequently, severe loss of vision as a result of complete loss of corneal epithelial stem cells. Transplantation of autologous corneal stem-cell sources is an alternative to allograft transplantation and does not require immunosuppression, but it is not possible in many cases in which bilateral disease produces total corneal stem-cell deficiency in both eyes. We studied the use of autologous oral mucosal epithelial cells as a source of cells for the reconstruction of the corneal surface.

METHODS

We harvested 3-by-3-mm specimens of oral mucosal tissue from four patients with bilateral total corneal stem-cell deficiencies. Tissue-engineered epithelial-cell sheets were fabricated ex vivo by culturing harvested cells for two weeks on temperature-responsive cell-culture surfaces with 3T3 feeder cells that had been treated with mitomycin C. After conjunctival fibrovascular tissue had been surgically removed from the ocular surface, sheets of cultured autologous cells that had been harvested with a simple reduced-temperature treatment were transplanted directly to the denuded corneal surfaces (one eye of each patient) without sutures.

RESULTS

Complete reepithelialization of the corneal surfaces occurred within one week in all four treated eyes. Corneal transparency was restored and postoperative visual acuity improved remarkably in all four eyes. During a mean follow-up period of 14 months, all corneal surfaces remained transparent. There were no complications.

CONCLUSIONS

Sutureless transplantation of carrier-free cell sheets composed of autologous oral mucosal epithelial cells may be used to reconstruct corneal surfaces and can restore vision in patients with bilateral severe disorders of the ocular surface.

From the Department of Ophthalmology, Osaka University Medical School, Osaka (K.N., Y.H., K.W., K.Y., N.M., H.W., Y.T.); the Institute of Advanced Biomedical Engineering and Science, Tokyo Women's Medical University, Tokyo (M.Y., S.N., A.K., T.O.); and the Department of Molecular Morphology, Kitasato University Graduate School of Medicine, Kanagawa (E.A.) — all in Japan. Address reprint requests to Dr. Nishida at the Department of Ophthalmology, Osaka University Medical School, Room E7, Yamadaoka 2-2, Suita, Osaka 565-0871, Japan, or at knishida@ophthal.med.osaka-u.ac.jp.

N Engl J Med 2004;351:1187-96.

CORNEAL EPITHELIAL STEM CELLS RE-side in the basal layer of the limbus,[1,2] the transitional zone between the cornea and the bulbar conjunctiva. These cells govern renewal of the corneal epithelium[3] by generating progeny (transient amplifying cells, which are cells committed to epithelial differentiation) with limited renewal capabilities that migrate from the limbus into the basal layer of the cornea.[4]

If corneal epithelial stem cells are completely absent owing to limbal disorder from severe trauma (e.g., thermal or chemical burns) or eye diseases (e.g., the Stevens–Johnson syndrome or ocular pemphigoid), then the sources of corneal epithelial cells have been exhausted, the peripheral conjunctival epithelium invades inwardly, and the corneal surface becomes enveloped by vascularized conjunctival scar tissue, resulting in corneal opacification that leads to severe visual impairment. Such pathological characteristics are considered to represent limbal stem-cell deficiencies.[5,6]

In patients with unilateral limbal stem-cell deficiency, autologous limbal transplantation is a method of surface reconstruction of the cornea.[7] This procedure, however, requires a large limbal graft from the healthy eye (incurring a risk of causing limbal stem-cell deficiency in the healthy eye[8]), and it is not possible in patients who have bilateral lesions.[9]

Limbal-allograft transplantation can be performed in patients with unilateral or bilateral deficiencies,[10] but it requires long-term immunosuppression that involves high risks of serious eye and systemic complications including infection and liver and kidney dysfunction.[10] In patients with the Stevens–Johnson syndrome or ocular pemphigoid, graft failure is common, even with immunosuppression, owing to serious preoperative conditions such as persistent inflammation of the ocular surface, abnormal epithelial differentiation of the ocular surface, severe dry eye, and lid-related abnormalities.[11-13]

To avoid allograft rejection and improve surgical outcome, some patients with unilateral stem-cell deficiencies have had corneal epithelial grafts constructed ex vivo by the expansion of autologous limbal stem cells harvested from healthy contralateral eyes and cultivated on cell carriers such as amniotic membranes[14,15] and fibrin gel.[16] This process, however, cannot be used for bilateral total limbal stem-cell deficiencies. Therefore, we studied an alternative replacement strategy for damaged corneal epithelium involving a tissue-engineered epithelial-cell sheet comprising only the patient's own oral mucosal epithelial cells. Transplantation of autologous oral mucosal epithelial cells cultured on amniotic membranes to a rabbit corneal model has recently been reported.[17,18]

We studied a new method of transplantation involving a carrier-free cell sheet by exploiting temperature-responsive culture surfaces. By lowering the temperature, we are able to detach all the cultured cells from the surfaces as an intact transplantable cell sheet, and any carrier or scaffold is excluded from the graft.[19] We report the results of ocular-surface reconstruction in four patients with the use of cultured autologous oral mucosal epithelial cells and carrier-free tissue-replacement sheets.

METHODS

SUBJECTS

This study was approved by the institutional review board of Osaka University Medical School, in Osaka, Japan. Oral and written informed consent were obtained from all patients. Patients with bilateral total limbal stem-cell deficiency were eligible for inclusion. Exclusion criteria included glaucoma or xerophthalmia (a skinlike appearance) of the entire ocular surface. Our results are for the first four consecutive patients enrolled, each of whom had one eye grafted with a tissue-engineered epithelial-cell sheet fabricated in culture from harvested autologous oral mucosal epithelial cells in our hospital from January 2003 through March 2003 (Table 1).

All grafted eyes had been clinically diagnosed as having total limbal stem-cell deficiency with complete disappearance of the palisades of Vogt (a radial infolding at the sclerocorneal junction and a biologic marker of the location of corneal epithelial stem cells) and complete coverage by fibrovascular in-growth from 360 degrees of the limbus over the entire cornea. All patients exhibited chronic conjunctival inflammation immunologically driven by the causative diseases reported previously,[20,21] despite therapy with topical steroids. Three of the four patients (Patients 1, 3, and 4) had severe deficiency of the tear film. Lid abnormalities, including chronic blepharitis, misdirection of the eyelashes, and keratinization of the posterior lid margin, contributed to poor ocular-surface conditions and were also noted in all eyes. Patients 1 and 4 had continuous inflammation with severe tear-film and lid abnormalities and keratinization of the ocular

Table 1. Preoperative Characteristics of Patients with Total Limbal Deficiency.

Patient No.	Age	Sex	Diagnosis	Eye	Ocular-Surface Condition			Previous Surgery	Other Eye Diseases
					Symblepharon*	Schirmer's Test without Topical Anesthesia†	Schirmer's Test with Nasal Stimulation‡		
	yr					*mm*			
1	58	M	Stevens–Johnson syndrome (chronic phase)	Right	+	1	2	Allogeneic corneal epithelium (cultivated on amniotic membrane) transplantation in 2000	None
2	69	M	Ocular cicatricial pemphigoid	Left	+	23	26	None	None
3	77	F	Ocular cicatricial pemphigoid	Right	+	1	1	Limbal transplantation with the use of amniotic membrane in 2001	Proliferative diabetic retinopathy, branch-retinal-vein occlusion
4	75	F	Ocular cicatricial pemphigoid	Right	+	1	2	Penetrating keratoplasty in 1999	None

* The plus sign indicates that symblepharon (adhesion of one or both eyelids to the eyeball) was found at the patient's ocular surface.
† Schirmer's test without anesthesia is a commonly used clinical test of lacrimal secretion (tearing). It is performed by measuring the amount of moisture on Whatman filter paper (5 mm by 35 mm) that is placed in the margin of the lower lid for five minutes. A value of less than 5 mm indicates impaired secretion.
‡ Schirmer's test with nasal stimulation is used to measure maximal tearing and is performed by inserting a cotton swab into the nasal cavity. A value of less than 10 mm indicates decreased tearing.

surface. Three of the four patients (Patients 1, 3, and 4) had previously undergone allogeneic grafting, which had failed within one year after surgery, despite systemic and local immunosuppression with cyclosporine (trough levels of 50 to 100 ng per milliliter).

Surgical procedures for all cell-sheet autografts were performed by the same surgeon. A complete ophthalmologic examination included measurement of best corrected visual acuity, slit-lamp biomicroscopy, tonometry, and indirect ophthalmoscopy and was performed in all patients every two to four weeks during the follow-up period, starting two weeks after transplantation. The assessments of visual outcomes were carried out by investigators who were not involved in performing the procedures and were not informed about which eye underwent transplantation or whether the assessment was preoperative or postoperative.

CULTURE AND FABRICATION OF AUTOLOGOUS ORAL MUCOSAL EPITHELIAL-CELL SHEETS

After each patient's oral cavity was sterilized with topical povidone-iodine, a 3-by-3-mm specimen of oral mucosal tissue was surgically excised from the interior buccal mucosal epithelium while the patient was under local anesthesia with xylocaine (Fig. 1A). Oral mucosal epithelial cells were collected by removing all epithelial layers after treatment with dispase II (3 mg per milliliter, Roche), at 37°C for one hour. Collected materials were placed in trypsin and EDTA for 15 minutes to form single-cell suspensions. Temperature-responsive cell-culture inserts (CellSeed) were prepared with the use of commercial cell-culture inserts (Falcon, Becton Dickinson) according to specific procedures described previously.[22] The temperature-responsive polymer poly(*N*-isopropylacrylamide), which reversibly alters its hydration properties with temperature, is chemically immobilized in thin films on cell-culture surfaces, facilitating cell adhesion and growth in normal culture conditions at 37°C. Reducing the temperature of the culture below 30°C causes this surface to hydrate and swell rapidly, prompting complete detachment of adherent cells without the use of typical proteolytic enzymes or treatment with EDTA. Confluent cell cultures on these surfaces can be conveniently harvested as a single, unsupported contiguous cell sheet, retaining cell-to-cell junctions as well as deposited extracellular matrix on the basal surface of the sheet.[23] Enzyme-free harvest permits the cell sheets to be readily manipulated, transferred, layered, or fabricated, because they adhere rapidly to other surfaces, such as traditional culture plastics,[22] other cell sheets, and tissues in vivo.[19]

To prepare lethally treated feeder layers, subconfluent NIH 3T3 cells were incubated with 16 μg of mitomycin C per milliliter for two hours at 37°C and then trypsinized and seeded onto tissue-culture wells (35-mm diameter, Becton Dickinson) at a density of 2×10^4 cells per square centimeter. Oral epithelial cells were separated from these feeder-layer cells during culture with temperature-responsive cell-culture inserts. We confirmed that multilayered cell sheets were fabricated only in the presence of 3T3 cells in the culture system. After culture in vitro for 14 days, epithelial-cell sheets (23.4 mm in diameter) were harvested by reducing the temperature to 20°C.

For colony-forming assays, treatment with trypsin and EDTA was used to isolate single cells from oral mucosal epithelium. Cells were counted, seeded onto culture dishes (35-mm diameter, Becton Dickinson), and cultured with feeder layers treated with mitomycin C. After cultivation for 10 to 12 days, dishes were fixed and stained with rhodamine B. Colony formation in the entire dish was screened under a dissecting microscope.

Figure 1 (facing page). **Transplantation of Autologous Tissue-Engineered Epithelial-Cell Sheets Fabricated from Oral Mucosal Epithelium.**

Panel A shows the removal of oral mucosal tissue (3 by 3 mm) from patient's cheek. Isolated epithelial cells are seeded onto temperature-responsive cell-culture inserts. After two weeks at 37°C, these cells grow to form multilayered sheets of epithelial cells. The viable cell sheet is harvested with intact cell-to-cell junctions and extracellular matrix in a transplantable form simply by reducing the temperature of the culture to 20°C for 30 minutes. The cell sheet is then transplanted directly to the diseased eye without sutures. In Panel B (the scale bar represents 50 μm), harvested cell sheets have three to five cell layers and do not resemble the original oral mucosa as shown in Panel C (the scale bar represents 100 μm) as closely as they resemble normal corneal epithelium as shown in Panel D (the scale bar represents 100 μm). Panel E shows a transmission electron micrograph of developed microvilli on the apical surface of the cell sheet. Specimens of human tissue-engineered epithelial-cell sheets harvested by reducing the temperature of the culture are immunostained green with anti–keratin 3 antibodies (Panel F), anti–β_1 integrin antibodies (Panel G), and anti-p63 antibodies (Panel H). The nuclei in Panels F, G, and H are shown in red. The scale bars represent 50 μm in Panels F, G, and H. The specimens in Panels B, C, and D are stained with hematoxylin and eosin.

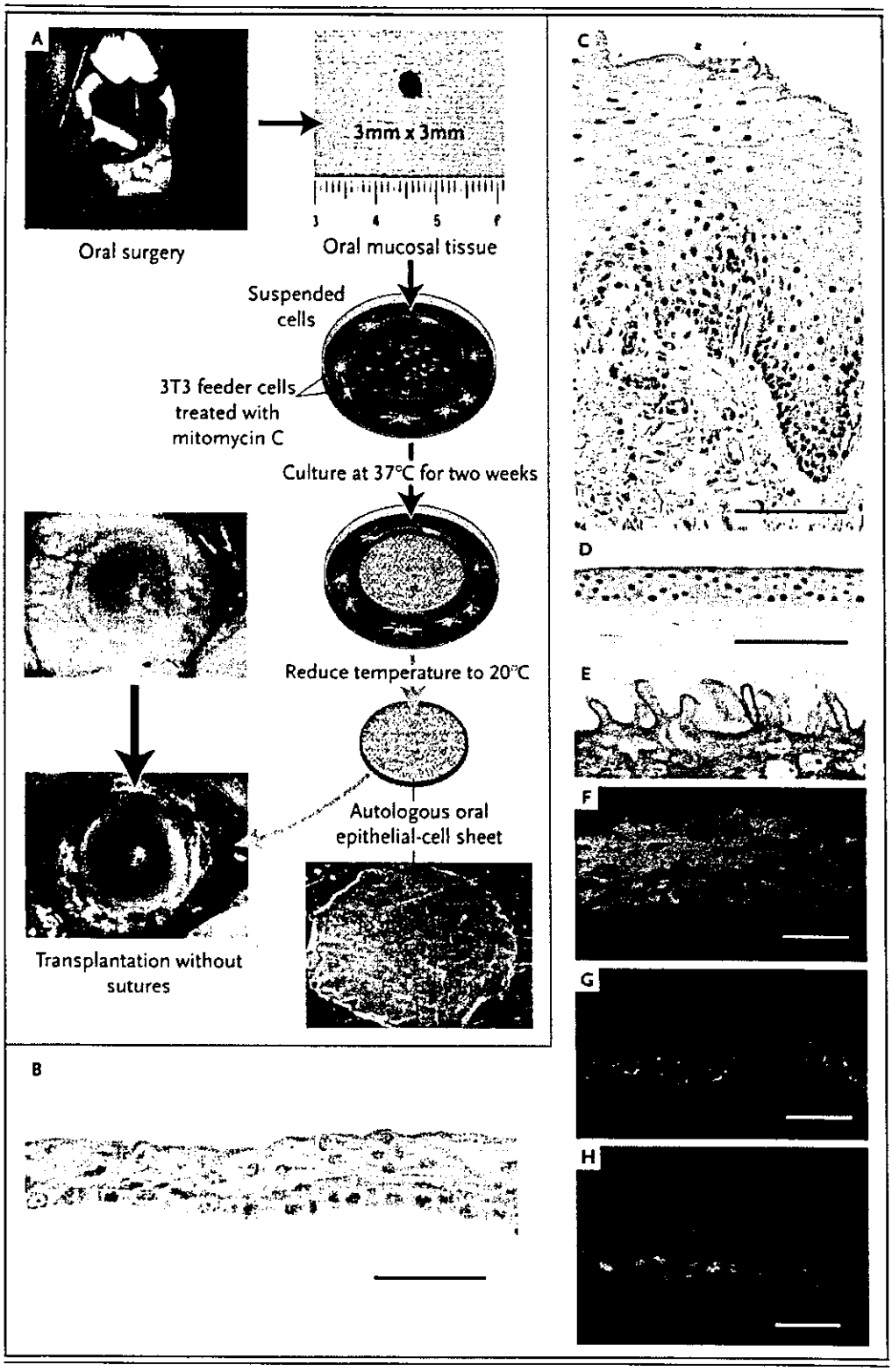
A
Oral surgery
3mm x 3mm
Oral mucosal tissue
Suspended cells
3T3 feeder cells treated with mitomycin C
Culture at 37°C for two weeks
Reduce temperature to 20°C
Autologous oral epithelial-cell sheet
Transplantation without sutures
B
C
D
E
F
G
H